NMR Evidence for Interconversion between Two Enantiomeric Forms of Macrocyclic Schiff Base Lanthanide(III) Complexes through Reversible Ring Contraction and Expansion

S. Aime,*,† M. Botta,† U. Casellato,‡ S. Tamburini,‡ and P. A. Vigato*,‡

Dipartimento di Chimica Inorganica, Chimica Fisica e Chimica dei Materiali, Università di Torino, Via P. Giuria 7, I-10125 Torino, Italy, and Istituto di Chimica e Tecnologie Inorganiche e dei Materiali Avanzati, CNR, Area della Ricerca, Corso Stati Uniti 4, I-35127 Padova, Italy

Received May 19, 1995[⊗]

Macrocyclic Schiff base lanthanide(III) complexes, $[Ln(H_2L_A)(NO_3)_2](NO_3)$ (Ln = Y^{3+}, La^{3+}, Nd^{3+}, Sm^{3+}, Eu^{3+}, Ho^{3+}, Yb^{3+}, Lu^{3+}), have been prepared by cyclocondensation of 2,6-diformyl-4-chlorophenol and 1,5-diamino-3-azapentane, in the presence of the appropriate metal nitrate as templating agent. In these complexes the metal ion occupies only one coordination site of the compartmental ligand, as evidenced by the X-ray structure of $[Y(H_2L_A)(NO_3)_2](NO_3)$. Crystals of this complex, grown from a dimethylformamide/diethyl ether solution, are monoclinic, space group *C*2/*c* [No. 15], with cell constants $a = 23.717(8)$ Å, $b = 14.651(7)$ Å, $c = 19.019(7)$ Å, and $\beta = 91.97(5)°$ for $Z = 8$. The yttrium atom is nine-coordinated, in a distorted tricapped trigonal prism environment formed by two bidentated nitrate groups and five donor atoms (two phenolic oxygens and three nitrogens) of the cyclic Schiff base H_2L_A. The third nitrate group is ionic. Metal–ligand interatomic distances: Y–O (nitrate), 2.48 Å (mean); Y–O (phenolic), 2.25 Å (mean). Variable-temperature proton and carbon NMR spectra of the diamagnetic Y(III), La(III), and Lu(III) complexes provide clear evidence for a novel chemical exchange process consisting of the reversible formation and breaking of an imidazole ring formed by the intramolecular nucleophilic attack of a secondary amino group at the imino carbon of a neighboring azomethine group. This dynamic process may be envisaged as a racemization of the enantiomeric forms of the structure found in the solid state. The basicity of the solvent appears to have a pronounced effect on the rearrangement rate. A direct role of the solvent is suggested in the N–H bond activation. The proton NMR spectra of the paramagnetic complexes $[Ln(H_2L_A)(NO_3)_2](NO_3)$ (Ln = Nd^{3+}, Sm^{3+}, Eu^{3+}, Ho^{3+}, Yb^{3+}) are consistent with the solution structure and dynamics found for the diamagnetic derivatives.

Introduction

The preparation and characterization of metal complexes with macrocyclic Schiff base ligands have been the subject of numerous studies in the recent past.[1–4] Macrocyclic Schiff bases have been prepared by the self-condensation reaction of appropriate keto or formyl and polyamine precursors, often through a template procedure. The presence of a suitable metal ion plays an important role in directing the synthetic pathway of the cyclic Schiff base formation.[5–7] Lanthanide(III) ions are effective template agents in the synthesis of [2+2] tetraimine macrocyclic Schiff bases, and several complexes have been characterized by X-ray diffractometry.[8–11] A ring contraction of the macrocyclic cavity has been observed, both in the free ligands and in the complexes, when there is a functional group (–NH or –OH) available for addition to the imine bond. Actually it was suggested, on the basis of a homonuclear proton 2D-COSY NMR experiment, that the macrocyclic Schiff base (H_2L_A) prepared by the [2+2] condensation of diethylenetriamine and 2,6-diformyl-4-chlorophenol consists of a mixture of three interconverting isomers as indicated in Figure 1.

Analogously, dealing with the Schiff base prepared by the [2+2] condensation of diethylenetriamine and *m*-phthalaldehyde, Martell and co-workers noted that the complexity of the ^1H and ^{13}C NMR spectra is indicative of the presence of a mixture of isomers, although the crystallization process selects only the 18-membered macrocycle containing two imidazolinic rings.[12,13] On the other hand, they suggested that, in the presence of 2 equiv of copper(II) ions, the equilibrium is probably completely shifted to the "open" form characterized by the absence of any imidazolinic ring.[12,13] Furthermore it was already reported that the structures of the Tb(III) and Eu(III) complexes $[(Ln(H_2L_A)(NO_3)_2](NO_3)$ contain the ligand in the contracted B-form.

On the basis of these observations, we were interested to assess whether the different dimensions of the coordinated metal ion may selectively orient the ring contraction or expansion. Thus we have prepared the trivalent rare earth complexes $[Ln(H_2L_A)(NO_3)_2](NO_3)$ (Ln = Y^{3+}, La^{3+}, Nd^{3+}, Sm^{3+}, Eu^{3+}, Ho^{3+}, Yb^{3+}, Lu^{3+}) by cyclocondensation of 2,6-diformyl-4-chlorophe-

† Università di Torino.
‡ CNR.
⊗ Abstract published in *Advance ACS Abstracts,* October 1, 1995.

(1) Fenton, D. E. In *Advances in Inorganic and Bioinorganic Mechanisms*; Sykes, A. G., Ed.; Academic Press: London, 1983; Vol. 2, p 187.
(2) Karlin, K. D.; Zubieta, J. *Biological and Inorganic Copper Chemistry*; Adenine Press: Guilderland, NY, 1986; Vols. 1 and 2.
(3) Willet, R. D.; Gatteschi, D.; Kahn, O. *Magneto-Structural Correlations in Exchange Coupled Systems*; NATO ASI Series; Reidel: Dordrecht, 1983.
(4) Guerriero, P.; Vigato, P. A.; Fenton, D. E.; Hellier, P. C. *Acta Chem. Scand.* **1992**, *46*, 1025.
(5) Lindoy, L. F.; Bush, D. H. *Preparative Inorganic Reactions*; Jolly, W. L., Ed.; Wiley-Interscience: New York, 1972; Vol. 6, p 2.
(6) Cook, D. H.; Fenton, D. E. *J. Chem. Soc., Dalton Trans.* **1979**, 266.
(7) Cook, D. H.; Fenton, D. E.; Rodgers, M. G. B.; McCann, A.; Nelson, S. M. *J. Chem. Soc., Dalton Trans.* **1979**, 414.
(8) Backer-Dirks, J. D. J.; Gray, C. J.; Hart, F. A.; Hursthouse, M. B.; Schoop, B. C. *J. Chem. Soc., Chem. Commun.* **1979**, 774.
(9) Abib, K. K.; Fenton, D. E.; Casellato, U.; Vigato, P. A.; Graziani, R. *J. Chem. Soc., Dalton Trans.* **1984**, 351.
(10) Smith, R. H.; Brainard, J. R.; Morris, D. E.; Jarvinen, G. D.; Ryan, R. R. *J. Am. Chem. Soc.* **1989**, *111*, 7437.
(11) De Cola, L.; Smailes, D. L.; Vallarino, L. M. *Inorg. Chem.* **1986**, *25*, 1729.
(12) Menif, R.; Martell, A. E.; Squattrito, P. J.; Clearfield, A. *Inorg. Chem.* **1990**, *29*, 4723.
(13) Drew, M. G. B.; Nelson, J.; Nelson, S. M. J. *J. Chem. Soc., Dalton Trans.* **1981**, 1678.

0020-1669/95/1334-5825$09.00/0

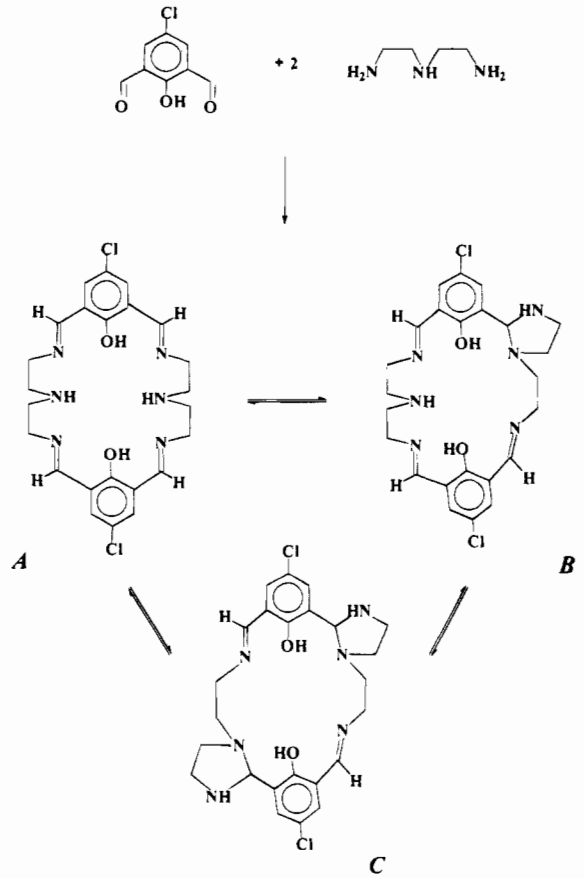

Figure 1. Schematic representation of the synthesis of the ligand H_4L_A and of its three interconverting isomeric forms.

nol and 1,5-diamino-3-azapentane, using the appropriate metal(III) trinitrate hexahydrate as templating agent, and studied their behavior in the solid state by X-ray diffractometry and in solution by variable-temperature ^1H and ^{13}C NMR spectroscopy.

To help better understand the spectroscopic data, the complex $[La(H_2L_B)(NO_3)_2](NO_3)$, where H_2L_B is the Schiff base obtained by condensation of 2,6-diformyl-4-chlorophenol and 1,5-diamino-3-methylazapentane, was prepared and its NMR spectra were investigated.

Experimental Section

Materials. 1,5-Diamino-3-azapentane, 1,5-diamino-3-azamethylpentane, $Ln(NO_3)_3{\cdot}6H_2O$ (Ln = Y^{3+}, La^{3+}, Nd^{3+}, Sm^{3+}, Eu^{3+}, Ho^{3+}, Yb^{3+}, Lu^{3+}), and the solvents were commercial products, used without further purification. 2,6-Diformyl-4-chlorophenol and the macrocycle H_2L_A were prepared and purified according to literature methods.[14-18] The elemental analyses of all the prepared complexes agree well with the proposed formulation.

$[Ln(H_2L_A)(NO_3)_2](NO_3)$ (Ln = Y^{3+}, Nd^{3+}, Sm^{3+}, Eu^{3+}, Ho^{3+}, Yb^{3+}, Lu^{3+}). The compounds were prepared by following literature procedures.[19] To a methanolic solution (20 mL) of 2,6-diformyl-4-chlorophenol (1 mmol) were added dropwise $Ln(NO_3)_3{\cdot}nH_2O$ (0.5 mmol) in methanol (10 mL) and 1,5-diamino-3-azapentane (1 mmol). The yellow or orange-yellow solution was refluxed for 2.5 h. The volume of the solution was reduced, and the yellow-orange precipitate obtained was filtered off, washed with diethyl ether, and dried in vacuo. After addition of a few drops of methanol to a warm dimethylformamide solution of the complex $[Y(H_2L_A)(NO_3)_2](NO_3)$, kept in an atmosphere saturated with diethyl ether, yellow crystals suitable for X-ray diffraction analysis were obtained.

Table 1. Summary of Crystallographic Data for $[Y(H_2L_A)(NO_3)_2](NO_3)$

formula	$YC_{24}H_{26}N_9O_{11}Cl_2$	V, Å^3	6605(2)
fw	776.33	Z	8
space group	$C2/c$ (No. 15)	D_{calc}, g/cm^3	1.56
a, Å	23.717(8)	μ(Mo Kα), cm^{-1}	19.34
b, Å	14.651(7)	temp, °C	295
c, Å	19.019(7)	$2\theta_{max}$, deg	50
β, deg	91.97(5)	λ, Å	0.7107
R^a	0.069	$R_w{}^b$	0.075

$^a R = \sum(|F_o| - |F_c|)/\sum|F_o|$. $^b R_w = (\sum w(|F_o| - |F_c|)^2/\sum w|F_o|^2)^{1/2}$.

$[La(H_2L_B)(NO_3)_2](NO_3)$. This compound was prepared by addition of $La(NO_3)_3{\cdot}6H_2O$ (0.5 mmol) in methanol (10 mL) and 1,5-diamino-3-methylazapentane (1 mmol) in methanol (10 mL) to a methanolic solution (20 mL) of 2,6-diformyl-4-chlorophenol (1 mmol). The resulting orange solution was refluxed for 2 h and then reduced in volume and allowed to stand overnight. The yellow-orange precipitate was collected by filtration, washed with a methanol/diethyl ether solution, and dried in vacuo.

Collection of Diffraction Data for $[Y(H_2L_A)(NO_3)_2](NO_3)$. Crystals of maximum dimension 0.3 mm were selected and used for X-ray analysis. The cell parameters and intensity data were collected on a Philips PW1100 automatic diffractometer (FEBO System), using graphite-monochromatized Mo Kα radiation (λ = 0.7107 Å) and the $\omega-2\theta$ scan method. Details are given in Table 1. The crystals were stable under irradiation, but their quality was very poor. Corrections were made for Lorentz–polarization and absorption effects.[20]

The structure was solved by direct methods. Owing to the paucity of observed reflections, anisotropy was introduced only for yttrium and chlorine atoms. The benzene rings were refined as rigid bodies. Hydrogen atoms bonded to carbons were introduced in the calculated positions with fixed C–H distances and isotropic temperature factors (C–H = 1.08 Å, U_{iso} = 0.082 Å^2). Refinement converged with R = 6.9%, R_w = 7.5% for 1391 reflections with $F > 4\sigma(F)$. Fractional coordinates and bond distances and angles are reported in Tables 2 and 3.

All calculations were carried out on a Digital ALPHA-AXP 300 computer using the programs SHELX-76 and SHELX-86.[21]

Physicochemical Measurements. IR spectra were recorded as KBr pellets on a Mattson FTIR 500 spectrometer equipped with a microscope.

^1H and ^{13}C NMR spectra were recorded on a Bruker AC200 spectrometer (200 MHz proton frequency) equipped with an Aspect3000 computer and on a JEOL EX400 spectrometer (400 MHz proton frequency). The resonances were assigned by conventional mono- and bidimensional techniques. All the samples examined were dissolved in hot dmso-d_6, pyridine-d_5, or $CDCl_3$, which also served as internal references.

Proton-detected [$^{13}C-^1H$] HSQC (homonuclear single-quantum coherence)[22,23] spectra with two purging spin-lock pulses to improve the suppression of signals of protons bound to ^{12}C were recorded on a Bruker AM 400, at 253 K, with no sample spinning. A 2 mM solution of $[Y(H_2L_A)(NO_3)_2](NO_3)$ in pyridine-d_5 contained in a 5 mm sample tube was utilized. The pulse sequence of Figure 2 was used: 200 experiments with SI = 2K, RD = 1 s, NS = 576, and DS = 4. Spectral widths of 6.024 kHz in f_2 with an acquisition time of 0.170 s and 20.0 kHz in f_1 with a final t_1 of 2.4 ms were utilized.

(14) Zinke, A.; Hanus, F.; Ziegler, E. *J. Prakt. Chem.* **1939**, *152*, 126.
(15) Taniguchi, S. *Bull. Chem. Soc. Jpn.* **1984**, *57*, 2683.
(16) Fironzabadi, H.; Mostafavipoor, Z. *Bull. Chem. Soc. Jpn.* **1983**, *56*, 914.
(17) Drago, R. S.; Desmond, M. J.; Carden, B. B.; Miller, K. A. *J. Am. Chem. Soc.* **1983**, *105*, 2287.
(18) Casellato, U.; Guerriero, P.; Tamburini, S.; Sitran, S.; Vigato, P. A. *J. Chem. Soc., Dalton Trans.* **1991**, 2145.
(19) Bünzli, J. C.-G.; Moret, E.; Casellato, U.; Guerriero, P.; Vigato, P. A. *Inorg. Chim. Acta* **1988**, *150*, 133.
(20) North, A. C. T.; Phillips, D. C.; Mathews, F. S. *Acta Crystallogr., Sect. A* **1968**, *24*, 351.
(21) Sheldrick, G. M. In *Crystallographic Computing 3*; Sheldrick, G. M., Kruger, C., Goddard, R., Eds.; Oxford University Press: London, 1985; p 175.
(22) Bodenhausen, G.; Ruben, D. J. *Chem. Phys. Lett.* **1980**, *69*, 185.
(23) Otting, G.; Wüthrich, K. *J. Magn. Reson.* **1988**, *76*, 569.

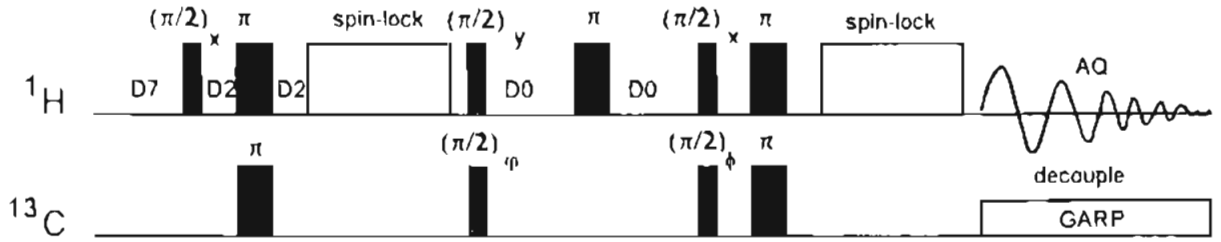

Figure 2. Pulse sequence HSQC.

Table 2. Fractional Coordinates and Isotropic (Atoms Denoted by *) or Equivalent Isotropic Thermal Parameters (Å^2)

atom	*x*	*y*	*z*	U_{iso}/U_{eq}[a]
Y(1)	0.63448(7)	0.5074(2)	0.1125(1)	0.0531(7)
Cl(1)	0.4016(2)	0.8668(4)	0.1850(4)	0.100(2)
Cl(2)	0.9507(2)	0.5739(5)	0.0499(3)	0.085(2)
N(1)*	0.6407(9)	0.467(1)	0.258(1)	0.093(5)
O(1)*	0.6434(6)	0.405(1)	0.2148(8)	0.083(4)
O(2)*	0.6315(6)	0.553(1)	0.2414(7)	0.076(4)
O(3)*	0.651(1)	0.456(2)	0.322(2)	0.195(6)
N(2)*	0.6246(7)	0.602(1)	−0.0192(9)	0.063(4)
O(4)*	0.5913(5)	0.5375(9)	−0.0035(7)	0.070(4)
O(5)*	0.6114(6)	0.664(1)	−0.0594(8)	0.083(4)
O(6)*	0.6718(5)	0.6047(9)	0.0175(7)	0.058(3)
N(9)*	0.864(1)	0.402(2)	−0.132(1)	0.137(6)
O(9)*	0.8466(9)	0.458(2)	−0.172(1)	0.160(6)
O(10)*	0.9097(8)	0.424(1)	−0.099(1)	0.117(5)
O(11)*	0.845(1)	0.335(2)	−0.128(1)	0.216(7)
N(3)*	0.5320(6)	0.494(1)	0.1401(7)	0.059(4)
N(4)*	0.5950(7)	0.353(1)	0.0752(9)	0.070(4)
N(5)*	0.7041(7)	0.404(1)	0.0502(9)	0.070(4)
N(7)*	0.7428(6)	0.755(1)	0.1710(8)	0.055(4)
N(8)*	0.6522(6)	0.802(1)	0.0911(8)	0.055(4)
O(7)*	0.6000(5)	0.6518(8)	0.1200(6)	0.052(3)
O(8)*	0.7211(5)	0.5461(8)	0.1519(6)	0.059(3)
C(3)*	0.5087(4)	0.8440(6)	0.1419(5)	0.057(5)
C(4)*	0.4592(4)	0.8016(6)	0.1623(5)	0.066(5)
C(5)*	0.4569(4)	0.7068(6)	0.1678(5)	0.056(5)
C(6)*	0.5041(4)	0.6543(6)	0.1528(5)	0.051(5)
C(1)*	0.5536(4)	0.6967(6)	0.1324(5)	0.049(4)
C(2)*	0.5559(4)	0.7916(6)	0.1270(5)	0.042(4)
C(7)*	0.4952(8)	0.557(1)	0.1533(9)	0.053(5)
C(8)*	0.5138(8)	0.398(1)	0.139(1)	0.067(5)
C(9)*	0.5307(8)	0.354(1)	0.075(1)	0.067(5)
C(10)*	0.6159(9)	0.326(2)	0.009(1)	0.087(6)
C(11)*	0.679(1)	0.323(2)	0.016(1)	0.101(6)
C(12)*	0.7567(8)	0.420(1)	0.043(1)	0.057(5)
C(14)*	0.8453(4)	0.4982(7)	0.0504(5)	0.060(4)
C(15)*	0.8810(4)	0.5681(7)	0.0744(5)	0.052(4)
C(16)*	0.8620(4)	0.6313(7)	0.1232(5)	0.048(4)
C(17)*	0.8075(4)	0.6246(7)	0.1479(5)	0.045(4)
C(18)*	0.7718(4)	0.547(7)	0.1238(5)	0.055(5)
C(13)*	0.7908(4)	0.4915(7)	0.0750(5)	0.060(5)
C(19)*	0.7873(8)	0.694(1)	0.198(1)	0.065(5)
N(6)*	0.7584(7)	0.653(1)	0.2601(9)	0.067(4)
C(20)*	0.7252(9)	0.734(1)	0.290(1)	0.084(5)
C(21)*	0.7263(8)	0.808(1)	0.233(1)	0.064(5)
C(22)*	0.7542(8)	0.806(1)	0.110(1)	0.063(5)
C(23)*	0.7036(7)	0.856(1)	0.079(1)	0.058(5)
C(24)*	0.6055(7)	0.843(1)	0.1076(9)	0.050(4)
N(10)*	0.500000	0.079(3)	0.250000	0.049(7)
C(25)*	0.529(2)	0.180(3)	0.244(3)	0.096(7)

[a] U_{eq} is defined as one-third of the trace of the orthogonalized U_{ij} tensor.

D2 (1.785 ms) was chosen for $J_{^1H-^{13}C}$ = 140 Hz. All ^{1}H pulses were produced using the decoupler; $\pi/2$ ^{13}C pulse length of 15.9 μs and spin-lock purge pulse of 2.5 μs at a power of 15.7 kHz were utilized. $\pi/2$ ^{13}C pulses of 9.5 μs were produced with the high-power transmitter. During the acquisition, ^{1}H decoupling was produced by a Bruker BFX5 device using a GARP sequence[24] and a low power, 100 μs, $\pi/2$ ^{13}C pulse. The raw data were processed on a Bruker X32 workstation with a digital resolution in f_1 of 0.5K; a sine square function with a phase shift of $\pi/3$ was applied in f_1, and a Gaussian function with LB = −5 and GB = 0.08, in f_2. The f_2 baseline was corrected with a third-order polynomial after the Fourier transform.

Table 3. Selected Bond Distances (Å) and Angles (deg) for $[Y(H_2L_A)(NO_3)_2](NO_3)$

Bond Lengths			
Y(1)−O(1)	2.45(2)	Y(1)−O(2)	2.54(1)
Y(1)−O(4)	2.44(1)	Y(1)−O(6)	2.49(1)
Y(1)−N(3)	2.51(1)	Y(1)−N(4)	2.54(2)
Y(1)−N(5)	2.56(2)	Y(1)−O(7)	2.27(1)
Y(1)−O(8)	2.24(1)		
Bond Angles			
O(7)−Y(1)−O(8)	94.1(4)	N(5)−Y(1)−O(8)	72.8(5)
O(4)−Y(1)−N(5)	86.9(5)	O(4)−Y(1)−O(7)	75.4(4)
O(1)−Y(1)−N(5)	88.2(5)	O(1)−Y(1)−O(8)	80.6(5)
O(1)−Y(1)−N(3)	81.0(5)	N(3)−Y(1)−O(7)	73.0(5)
O(4)−Y(1)−N(3)	79.9(4)	O(2)−Y(1)−O(6)	125.4(5)
O(2)−Y(1)−N(4)	118.2(5)	O(6)−Y(1)−N(4)	116.4(5)
O(1)−Y(1)−O(2)	52.7(5)	O(4)−Y(1)−O(6)	52.3(4)

The homogeneity of the complexes was checked with a Philips SEM XL40 scanning electron microscope, equipped with an EDAX PV99 X-ray energy dispersive spectrometer. The chlorine/lanthanide ratios were also determined by energy dispersive X-ray spectrometry (EDX).

The solvent content (H_2O or MeOH) was evaluated by thermal analysis curves using a Netzsch STA 429 thermoanalytical instrument. The tests were performed in a nitrogen atmosphere (flux rate 250 mL/min; heating rate 5 °C min^{-1}) and in air under the same conditions. Neutral alumina (Carlo Erba Products) was used as reference material. X-ray diffraction patterns were recorded by the transmission technique, using a Philips X'PERT instrument operating in the Bragg−Brentano geometry using a NaI(Tl) scintillation counter diffractometer; Cu Kα radiation was employed. The step-scanning recording was performed in the 5−60° (2θ) range at 0.002° steps and with a counting time of 15 s per step.

Results and Discussion

Preparation and Properties of the Complexes. The complexes $[Ln(H_2L_A)(NO_3)_2](NO_3)$ were prepared by condensation in methanol of equimolar amounts of 2,6-diformyl-4-chlorophenol and 1,5-diamino-3-azapentane, in the presence of $Ln(NO_3)_3{\cdot}6H_2O$ as a templating agent. The complexes are yellow solids, stable in air, and do not incorporate solvent molecules. The cyclic nature of the ligand was suggested by the presence of strong absorptions due to C=N at 1662−1665 cm^{-1} and by the absence of bands due to $\nu_{C=O}$ or ν_{NH_2}. Moreover, bands at 1460−1466, 1301−1266, 1038−1027, and 820−817 cm^{-1} due to bidentate nitrate groups are also detectable in addition to a band at $\simeq$ 1386 cm^{-1} attributable to ionic NO_3^-.

In a similar way, $[La(H_2L_B)(NO_3)_2](NO_3)$ was prepared by condensation of 2,6-diformyl-4-chlorophenol and 1,5-diamino-3-methylazapentane, in the presence of the appropriate $Ln(NO_3)_3{\cdot}6H_2O$ as templating agent. The infrared spectra of this complex parallel those of $[Ln(H_2L_A)(NO_3)_2](NO_3)$, indicating almost identical coordinations about the central metal ion. Attempts to introduce a second (same or different) rare earth

(24) Shaka, A. J.; Barker, P. B.; Freeman, R. *J. J. Magn. Reson.* **1985**, *64*, 547.

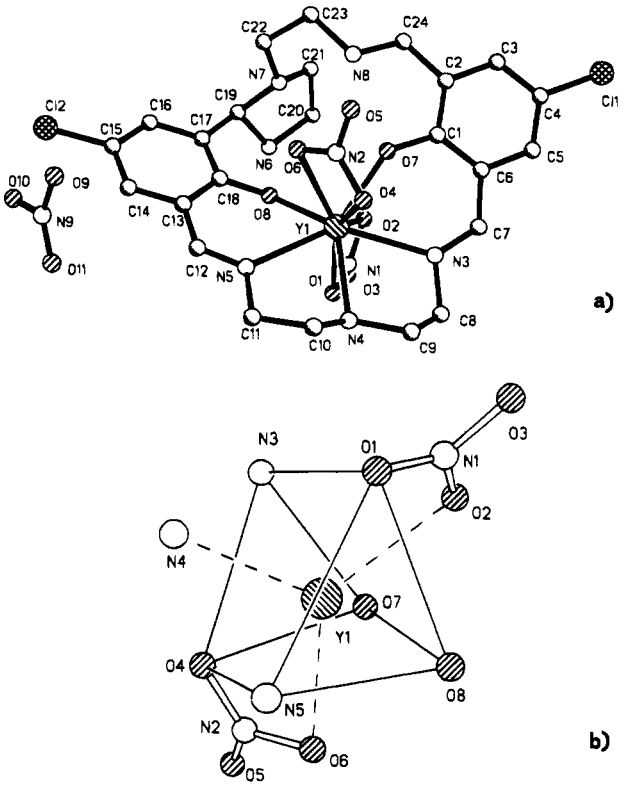

Figure 3. (a) Perspective drawing of $[Y(H_2L_A)(NO_3)_2](NO_3)$ showing the atom-numbering scheme. (b) Coordination polyhedron around the yttrium atom.

ion into the free coordination chamber failed. Invariably, the starting complex was recovered. Also, when elemental analyses suggested the formation of unlikely di- or trinuclear species, electron microscopy and EXD investigations showed that the samples were not homogeneous; i.e., we had obtained mononuclear complexes contaminated by hydrolytic products.

Further purification or recrystallization of these mixtures leads to the formation of the pure mononuclear complexes $[Ln(H_2L_A)(NO_3)_2](NO_3)$. During recrystallization of the crude complexes, only $[Y(H_2L_A)(NO_3)_2](NO_3)$ provided crystals suitable for X-ray diffraction study. Powder X-ray investigations revealed that all $[Ln(H_2L_A)(NO_3)_2](NO_3)$ complexes considered in this work are isostructural.

The complexes are sparingly soluble in noncoordinating solvents, such as $CHCl_3$, and show a moderate solubility in coordinating solvents, such as pyridine, dimethylformamide, or dimethyl sulfoxide. The compositions of the complexes recovered after their dissolution in these solvents do not suffer appreciable variations. In fact, from these solutions, after removal of the coordinating solvents by evaporation at reduced pressure, the starting complexes $[Ln(H_2L_A)(NO_3)_2](NO_3)$ were recovered.

Crystal Structure of $[Y(H_2L_A)(NO_3)_2](NO_3)$. The complex crystallized in the monoclinic space group *C2/c* [No. 15]. Each unit cell contains 8 molecules. The closest intermolecular contacts (3.21(3) Å) are those between C(11) and O(11) atoms. The macrocycle displays a type-B structure (Figure 1) consisting of an 18-membered inner ring and a 5-membered imidazoline outer ring. The yttrium atom is nine-coordinated; the coordination polyhedron can be described as a distorted tricapped trigonal prism where two nitrate groups are coordinated as bidentate ligands and five donor atoms (two phenolic oxygens and three nitrogens) of the cyclic polydentate ligand complete the coordination prism, in which N(4) (amine), O(2) (nitrate), and O(6) (nitrate) are the caps, as shown in Figure 3b.

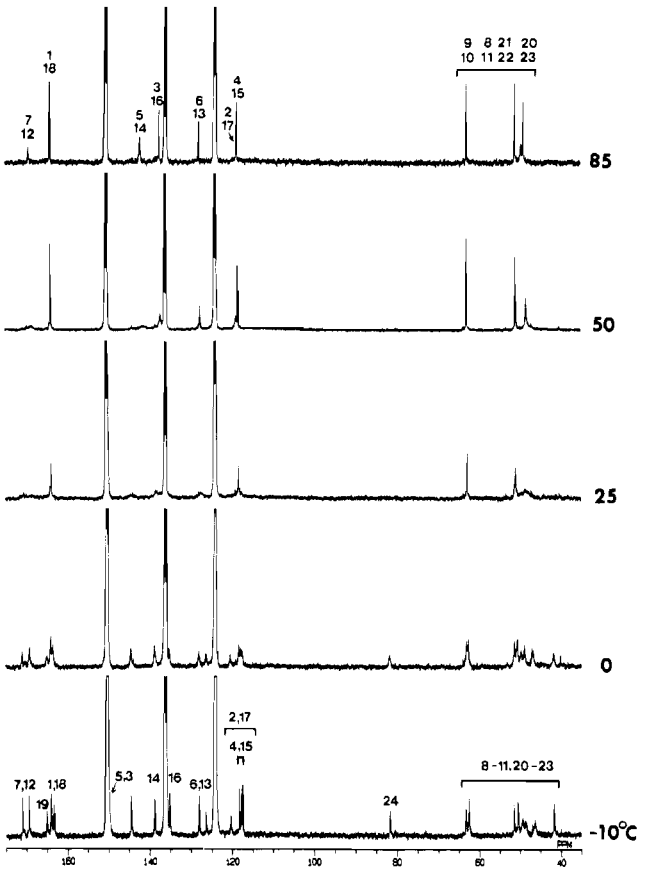

Figure 4. Variable-temperature 100 MHz $\{^1H\}^{13}C$ NMR spectra in pyridine-d_5 for $[La(H_2L_A)(NO_3)_2](NO_3)$. The resonances have been labeled according to Figure 5.

The third nitrate group is ionic. Three types of metal−ligand interatomic distances have been found: Y−O (nitrate), 2.48 Å (mean); Y−O (phenolic), 2.25 Å (mean); Y−N, 2.54 Å (mean). The apparent discrepancy that the Y−O (nitrate, charged) distances are longer than the Y−O (phenolic, neutral) distances is explained by the different geometries of the ligands, as already discussed in previous papers for the isostructural terbium(III) and europium(III) complexes[19,25] (Figure 3).

Thus, as in the case of Tb(III) or Eu(III) complexes, the metal ion occupies only one chamber of the macrocycle. The other chamber is not involved in the coordination and displays a ring closure.

Other structural details are normal and comparable with those reported for the structures of Tb(III) or Eu(III) complexes.

Solution Structures and Dynamics of $[Ln(H_2L_A)(NO_3)_2](NO_3)$ Complexes (Ln = Y^{3+}, La^{3+}, Lu^{3+}). According to the X-ray structure, all the carbon atoms of the $La(H_2L)(NO_3)_3$ complexes are stereochemically and magnetically different, and thus 24 different resonances are expected in their ^{13}C NMR spectra. As shown in Figure 4, 23 resonances are clearly detected in the spectrum of the La(III) derivative, at −10 °C in pyridine-d_5 δ_C (ppm) = 41.77, 46.63, 48.91, 49.70, 50.59, 51.41, 62.62, 63.21, 81.74, 117.46, 117.76, 118.28, 120.40, 126.26, 127.99, 135.13, 138.78, 144.49, 163.45, 164.09, 164.98, 169.31, 170.99). The remaining resonance is masked by the intense solvent peak at 150.21 ppm. The assignment of the resonances has been possible, on the basis of their proton-coupled pattern, by the comparison with literature values for related compounds and by their variable-temperature (VT) behavior (vide infra).

(25) Casellato, U.; Guerriero, P.; Tamburini, S.; Vigato, P. A.; Graziani, R. *Inorg. Chim. Acta* **1987**, *129*, 127.

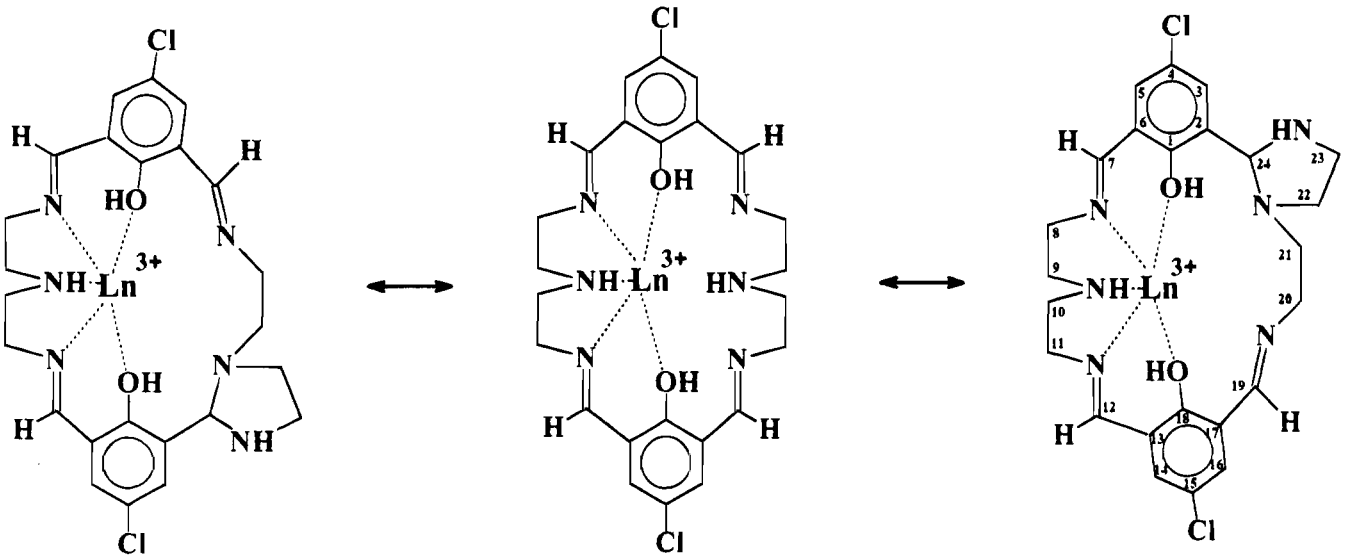

Figure 5. Ring contraction and expansion process for $[Ln(H_2L_A)(NO_3)_2](NO_3)$.

Then, the low-temperature ^{13}C NMR limiting spectrum unambiguously indicates that also in the case of the La(III) complex the macrocyclic ligand adopts, in solution, a B-type structure.

As the temperature is increased, all the resonances broaden, collapse into the baseline near room temperature, and merge again, above 70 °C, to give pairs of two-by-two averaged signals. Only the average signal corresponding to the pair C(19)/C(24) has not yet merged in the spectrum recorded at 85 °C.

The reduction from 24 to 12 resonances in the high-temperature limiting spectrum clearly suggests that a dynamic process is occurring in this temperature range. The observed exchange pathway is indicative of an equilibration process of the kind depicted in Figure 5, which involves reversible ring contraction and expansion.

The VT ^1H NMR spectra of $La(H_2L_A)(NO_3)_3$ fully support the above conclusions. The low-temperature limiting spectrum shows two sets of aromatic resonances (proton pairs H(5)/H(14) at 7.37 and 7.31 ppm and H(3)/H(16) at 7.35 and 7.24 ppm, at −10 °C) which are averaged out at high temperature. The clue to the exchange mechanism is represented by the averaging process involving H(19) and H(24) (δ_H (ppm) = 8.72 and 3.22, respectively, at −10 °C) which has been confirmed by a 2D-EXSY experiment. The ethylenic region is more complex, but at high temperature it unambiguously corresponds to two AA′BB′ spin systems. The values for the activation parameters of the dynamic process were obtained from the analysis of the VT carbon spectra by the following procedure: (a) the rate constants k at the coalescence temperatures T_c for five pairs of exchanging resonances were calculated by the equation

$$k = \pi\Delta\nu/\sqrt{2} \qquad (1)$$

where $\Delta\nu$ is the separation in hertz between the exchanging resonances in the absence of exchange (spectrum at −10 °C);[26] (b) from the plot of $\log(k/T)$ against $1/T$ the enthalpy of activation $\Delta H^{\ddagger}$ and the entropy of activation $\Delta S^{\ddagger}$ were evaluated.[26]

The following results were obtained: $\Delta H^{\ddagger} = 80.0 \pm 1.6$ kJ mol^{-1} and $\Delta S^{\ddagger} = 75.2 \pm 12$ J mol^{-1} K^{-1}, which correspond at 298 K to a $\Delta G^{\ddagger}$ value of 57.6 ± 2.4 kJ mol^{-1}.

(26) Friebolin, H. *Basic One- and Two-Dimensional NMR Spectroscopy*, 2nd ed.; VCH Publishers: Weinheim, Germany, 1993; pp 293−296.

Strictly analogous features are shown by the proton NMR spectra of the Lu(III) complex: the four separate resonances (δ_H (ppm) = 7.42−7.57), corresponding to protons H(5)/H(14) and H(3)/H(16), which are clearly detectable at temperatures <−10 °C, coalesce at ~5 °C and produce two peaks of relative intensity 2 at higher temperatures. These data qualitatively indicate similar activation energies for the dynamic processes of the complexes with the lighter and heavier members of the lanthanide series, which in turn implies a limited dependence of the observed effects on the ionic size. Unfortunately, a more quantitative analysis was precluded by the very poor solubility (<3 mg/cm^3) of the Lu(III) complex, which did not allow us to carry out a VT ^{13}C NMR study. However, a carbon spectrum, recorded after 52 h of accumulation at 50 °C, closely parallels the analogous spectrum of the La(III) derivative in both number of peaks and bandwidth due to exchange broadening effects, in agreement with the conclusion derived from the proton data.

Definitive proof that the dynamic behavior corresponds to the reversible cleavage and formation of the imidazoline group was obtained by substituting 1,5-diamino-3-azopentane with 1,5-diamino-3-methylazapentane in the template synthesis of the macrocyclic La(III) complex. The methyl substitution at the secondary amino groups prevents the formation of the imidazoline ring. In this complex, the ligand is then in a type-A conformation (Figure 1) as evidenced by the four narrow resonances in the low-field region (δ_H (ppm) = 8.69, 8.29, 7.73, 7.68; in CD_3OD at 25 °C) of its ^1H NMR spectrum, corresponding to a highly symmetrical structure. Interestingly, the complex appears to be stereochemically rigid on the NMR time scale, in spite of the availability of two identical coordination chambers.

Finally, we decided to investigate the ^{13}C NMR spectrum of $[Y(H_2L_A)(NO_3)_2](NO_3)$ to assess whether the structure found in the solid state was maintained in solution. Direct observation of the carbon spectrum was impossible because of the extremely low solubility of this complex. We turned then to a 2-D-heterocorrelated reverse experiment by using a pulse sequence developed by Otting and Wüthrich.[22−24] This experiment allowed the indirect detection of the ^{13}C spectrum that was very similar, in both number and position of the resonances, to that reported above for the corresponding La(III) complex. In Figure 6 is shown the low-temperature aliphatic carbon region where, in particular, one can clearly observe a cross peak correlating

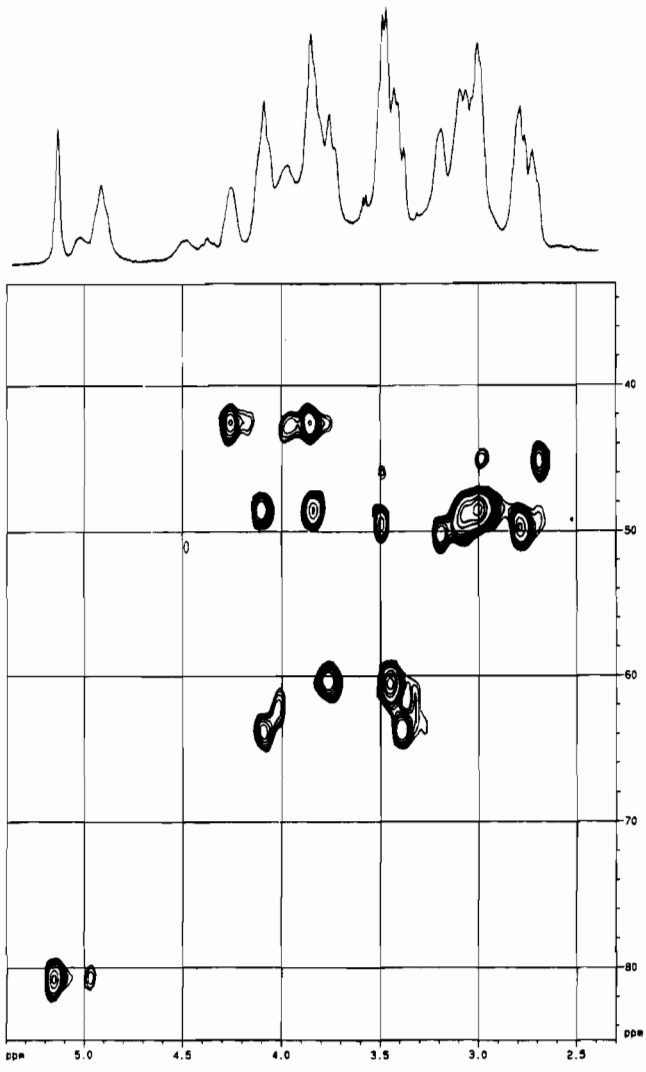

Figure 6. Expanded region of the [^{13}C−^{1}H] HSQC spectrum for a 2 mM pyridine-d_5 solution of $[Y(H_2L_A)(NO_3)_2](NO_3)$ at 243 K.

the proton peak at 5.16 ppm and a carbon resonance at 81 ppm, diagnostic of the contracted form of the complex.

This result allows us to conclude that the solid state structure closely corresponds to the solution structure in the low-temperature limiting spectrum. The VT behavior of the ^{1}H NMR spectra of the yttrium(III) derivative (in pyridine-d_5) suggests the same rearrangement, with similar activation energy, inside the macrocyclic ligand shown by the analogous diamagnetic La(III) and Lu(III) complexes.

Effects of the Basicity of the Solvent on the Intramolecular Rearrangement. The solvent appears to have a marked effect on the rearrangement, as found in comparing the ^{1}H NMR spectra of the Y(III) complex recorded in pyridine, methanol, and dimethyl sulfoxide at the same temperature (298 K). In this regard, the appearance of the low magnetic field region is particularly diagnostic. In the more basic pyridine, the spectral pattern consists of three sharp resonances (two of them partially overlapping with the central peak of C_5D_4NH solvent), thus indicating the occurrence of a fast-exchange situation.

On the other hand, in CD_3OD the same spectral region shows six, relatively narrow resonances as expected in the case of a "frozen" structure. The exchange in DMSO-d_6 is intermediate, and the aromatic resonances appear very broadened.

The observed behavior clearly suggests a direct role of the solvent in promoting the rearrangement of the macrocycle. We propose that the intermediacy of the solvent occurs by favoring

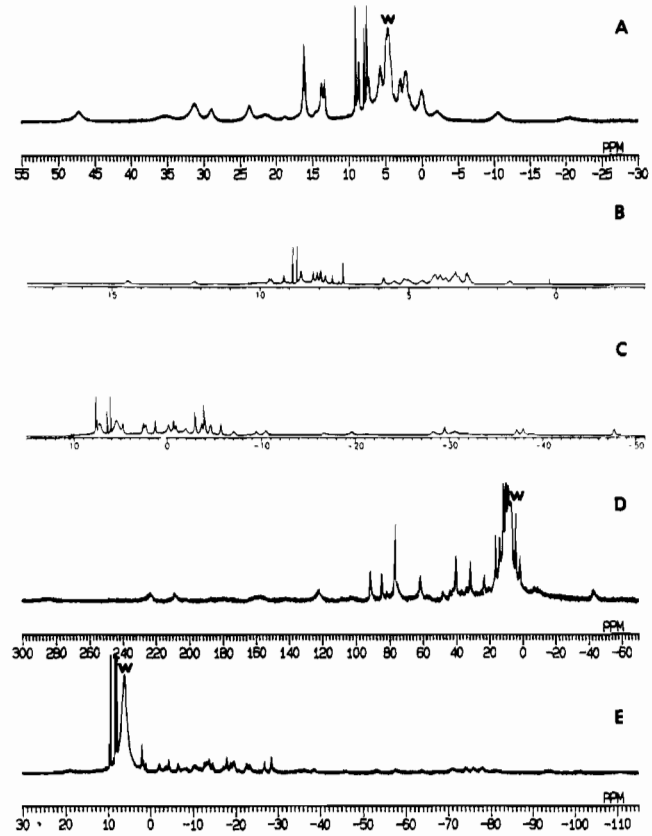

Figure 7. ^{1}H NMR spectra in pyridine-d_5 of $[Ln(H_2L_A)(NO_3)_2](NO_3)$: (A) Ln = Nd, 90 MHz, 258 K; (B) Ln = Sm, 200 MHz, 235 K; (C) Ln = Eu, 200 MHz, 250 K; (D) Ln = Ho, 90 MHz, 258 K; (E) Ln = Yb, 90 MHz, 253 K. The intense peak labeled with "w" refers to the water signal.

the proton−nitrogen cleavage of the imidazoline ring, followed by successive protonation at the central nitrogen. Then a ring contraction occurs through the formation of a new imidazoline ring on the other side of the compartment. Thus the most basic pyridine appears the most efficient solvent in catalyzing the intramolecular rearrangement. Interestingly, during the step of ring expansion, the Ln(III) ion remains tightly bound and is not involved in any exchange between the two compartments.

Solution Structures of the Paramagnetic Ln(III) Complexes $Ln(H_2L_A)(NO_3)_2$ (Ln = Nd, Sm, Eu, Ho, Yb). In Figure 7 we report the low-temperature limiting ^{1}H NMR spectra in pyridine-d_5 of five $[Ln^{III}(H_2L_A)(NO_3)_2](NO_3)$ complexes (Ln = Nd, Sm, Eu, Ho, Yb). As one can see, they span over very different range of chemical shift values, as expected on the basis of the differences in their magnetic moments μ_{eff} and in the relative contributions of the contact and dipolar components of the paramagnetic shift. However, the large number of resonances observed at low temperature is consistent with the occurrence of the structure found in the solid state for the Tb(III), Eu(III), and Y(III) complexes. On this basis, a partial assignment of the ^{1}H NMR spectra becomes possible. In fact, in all five spectra, one may recognize two groups of resonances each roughly accounting for half of the overall spectral intensity. One group is composed of broad and more shifted (from the diamagnetic region) resonances which are then assigned to protons belonging to the compartment containing the paramagnetic ion, while the other group is formed by relatively sharp and less shifted resonances corresponding to proton nuclei on the uncoordinated compartment of the macrocycle.

For all five complexes, the increase in temperature invariably leads to overall broadening and subsequent collapse of the resonances. The spectra at the highest obtainable temperature

display a decreased number of resonances to indicate that a dynamic process is taking place. This behavior is particularly evident for the set of less shifted resonances and for the whole spectrum of the Sm(III) complex which covers a region of about 15 ppm. Although the complexity of the observed spectral pattern of the ^{1}H NMR spectra for the paramagnetic complexes prevents acquiring further insight into the dynamic processes, it appears likely that the observed spectral changes with the increase of temperature are fully consistent with the rearrangement described above for the diamagnetic derivatives.

Conclusions

Most of the observations reported in this paper lead to the conclusion that the coordination of Ln(III) ions (Ln = Y, La, Tb, Eu, Lu) invariably involves the B-type structure of the macrocyclic ligand. Furthermore the VT-NMR studies clearly indicate an extensive rearrangement of the ligand on the NMR time scale. This dynamic process occurs through C−N bond activation and a hydrogen transfer mechanism, resulting in reversible ring contraction and expansion. This novel type of stereochemical nonrigid behavior provides a fast enantiomerization pathway for the B-type complexes considered in this work. Thus, although the coordination mode of the macrocyclic ligand often gives rise to enantiomeric complexes, it is not straightforward to show their occurrence by spectroscopic means. This appears to be an interesting case where the presence of enantiomeric forms is revealed through the elucidation of the underlying exchange process.

The interconversion between contracted and uncontracted forms of the macrocycle is reminiscent of the labile nature of the Schiff bases formed in solution. In fact, this feature explains their ability to interconvert from linear (kinetically favored) to cyclic (thermodynamically favored) forms. In turn, this rearrangement occurs intramolecularly in the macrocyclic Schiff base for the compartment not involved in the coordination bonding scheme.

Acknowledgment. We thank Mrs. O. Biolo, Mr. E. Bullita, and Mrs. A. Moresco for experimental assistance and Prof. S. Mammi for the 2D HSQC experiment. The support of Progetto Strategico—CNR—Tecnologie Chimiche Innovative is also gratefully acknowledged.

Supporting Information Available: Figure S1, showing an Eyring plot for the exchange of correlated pairs of carbon resonances, and Tables S1−S5, listing X-ray experimental details, anisotropic thermal parameters, hydrogen fractional coordinates, bond distances, and bond angles (8 pages). Ordering information is given on any current masthead page.

IC950612Y